

DNA-programmable particle superlattices: Assembly, phases, and dynamic control

Oleg Gang and Alexei V. Tkachenko

Nanoparticles (NPs) have emerged as new functional blocks for optical, energy, and biomedical applications, opening a new frontier of rational self-assembly of materials. One of the most controllable assembly strategies relies on programming interparticle interactions using the complementarity of DNA strands, providing selective and reversible interactions between particles of different sizes and shapes. Much progress has been achieved in DNA-guided assembly of particle superlattices. By tuning the interactions, sizes, and shapes of NPs, a wide variety of structures have been assembled. This article discusses the most significant achievements and challenges in assembly of DNA-programmable particle superlattices.

Introduction

The field of colloidal assembly was driven for a long time by fundamental interest in understanding crystallization in simple model systems. More recently, colloids and their nanoscale analogs, nanoparticles (NPs), have emerged as new functional blocks for optical, energy, and biomedical applications. These developments have opened a new frontier of rational self-assembly of materials made from such particles. The structures of the assemblies are determined by the interplay among interaction forces, entropic effects, and kinetics. Unlike atoms, colloids and NPs can vary widely in their sizes, shapes, and interactions. Nevertheless, it has been challenging to establish a broadly applicable platform for "a la carte" assembly of ordered particle arrays and their dynamic control.[1–3]

One of the most controllable assembly strategies relies on programming interparticle interactions using the complementarity of DNA strands.[3] This provides selective and reversible interactions between particles of different sizes and shapes (**Figure 1**). DNA strands can also act as tailored structural elements in particle crystals, smart assembly guides, and reconfigurable structural elements. In recent years, much progress has been made in DNA-guided assembly of particle superlattices. By tuning the interactions, sizes, and shapes of NPs, a wide variety of structures have been assembled. Here, we discuss the most significant achievements and challenges in this field and future directions.

Crystallization of superlattices

DNA was proposed as a programmable "glue" for the assembly of NPs about two decades ago.[8,9] The basic idea is that DNA-functionalized NPs with complementary strands can hybridize due to the Watson–Crick base pairing between the strands grafted to two different particles. One can consider two approaches to link particles with DNA: direct hybridization (DH) and linker-mediated hybridization (LH) (see Figure 1). In the DH approach, the particles are functionalized by DNA terminated with mutually complementary single-stranded segments (also known as a "sticky end"). In the LH approach, the grafted DNA pairs are not complementary, and appropriately encoded DNA linkers are required to connect them. In addition, the grafted DNA can vary in their rigidity, length, and grafting density, all of which lead to modification of the shell, formed by DNA around the particle core, and, consequently, it will affect particle interaction characteristics.

DNA-mediated particle binding without additional optimization or annealing would normally lead to amorphous aggregates due to unfavorable interactions and complex kinetic pathways to crystallization.[10,11] Crocker's group reported the first example of crystallization for DNA-coated particles for micrometer-scale colloids[12] (see formation of small crystallites in **Figure 2**a–c). The Gang[13,14] and Mirkin[15] groups independently reported a major breakthrough, an assembly of crystalline 3D lattices from NPs using DNA.

Oleg Gang, Center for Functional Nanomaterials, Brookhaven National Laboratory, USA; ogang@bnl.gov
Alexei V. Tkachenko, Center for Functional Nanomaterials, Brookhaven National Laboratory, USA; oleksiyt@bnl.gov
doi:10.1557/mrs.2016.92

© 2016 Materials Research Society

https://doi.org/10.1557/mrs.2016.92 Published online by Cambridge University Press

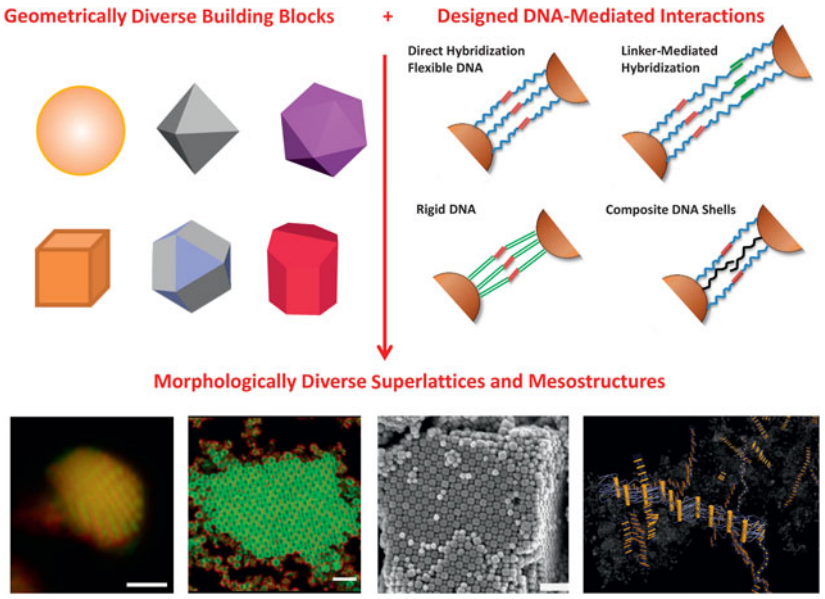


Figure 1. Schematic representation of the concept of DNA-mediated programmable self-assembly of particles. Particles can be coated with DNA shells, thus, the particle cores carry materials function, and DNA shells provide programmable interactions. (Top left panel): the diversity of particle shapes that can be synthesized. (Top right panel): richness of DNA-shell designs for modulating DNA-driven interparticle interactions. (Bottom panel): from left to right, crystallization of colloid particles,[4] binary mixture of colloid particles,[5] nanoscale cubes and spheres,[6] and a symmetry breaking for DNA-interacting rods due to the collective chain effect results in a ribbon formation.[7] Note: Scale bars, from left to right, are 2 μm, 5 μm, and 200 nm. Reprinted with permission from References 4 and 5. © 2012 and 2015 Macmillan Publishers Ltd.

The key advances were (1) the use of a thermal annealing procedure combined with *in situ* small-angle x-ray scattering for sample structure monitoring; and (2) rational design of the DNA shell to optimize the interparticle interactions. The optimal temperature window for the onset of crystallization was shown to be about a few degrees below the DNA melting temperature.

Theory[16] suggested that order requires a particular balance of attraction and repulsion, which can be controlled by the design of the DNA shell, for example, through manipulating the DNA rigidity[13] and mixing different strand types.[11,17] Utilizing these approaches, the crystallization of NPs into body-centered-cubic (bcc) or face-centered-cubic (fcc) phases was achieved.[13–15] The fcc phase was formed from single-type particles (all particles in the system have the same DNA shell), while the bcc phase (isostructural to CsCl) (i.e., presence of two types of species in the lattice) was observed in binary particle systems (particles with two types of DNA) with mutual attraction, consistent with earlier theoretical predictions.[16] A systematic study[14,18] of LH NP systems identified the minimum number of DNA linkers required for robust crystallization, which was later confirmed by Monte Carlo simulations in which DNA shells were modeled as "soft colloids."[19] Experiments indicated that phase behavior was sensitive to the details of shell tailoring,[4] and the morphology of assembly could be kinetically tuned.[20,21]

Theory and modeling of DNA-driven particle systems

From a theoretical point of view, particles with DNA-mediated particle binding represent a unique model system with designed interactions and a significant methodological challenge due to its multiscale character. The theoretical and computational approaches for describing DNA-mediated particle interactions can be roughly divided into three groups: (1) models in which the DNA subsystem is replaced with effective pair potential; (2) simulations with explicit coarse-grained polymer models of DNA; and (3) hybrid approaches in which simulations of chains are used for the effective potential (EP).

The EP models were among the first proposed.[16,22,23] In general, the EP is well justified primarily for the colloids, which are larger than typical DNA shells. Fundamentally, these potentials can be calculated as a free energy of the DNA

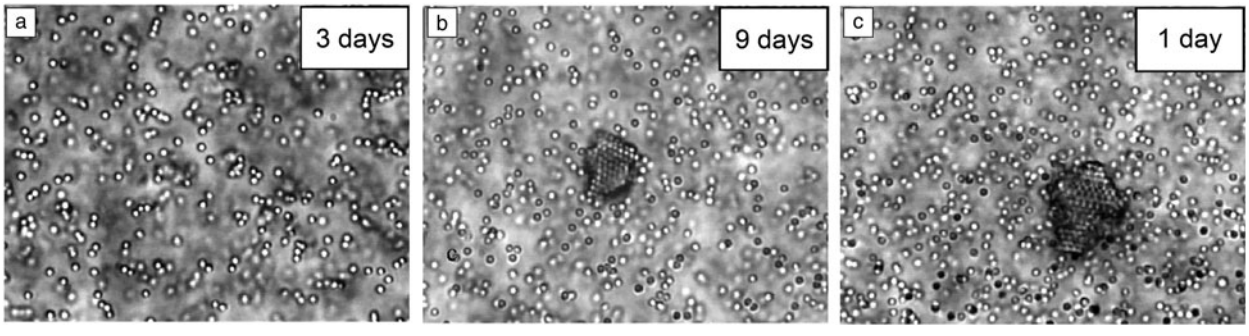


Figure 2. Crystallization results for 1-μm diameter DNA-grafted colloidal particles after (a) three days (~1500 DNA/particle), (b) nine days (~1500 DNA/particle), and (c) one day (~9500 DNA/particle). Particles are 1 μm in diameter. Reprinted with permission from Reference 12. © 2006 American Chemical Society.

https://doi.org/10.1557/mrs.2016.92 Published online by Cambridge University Press

subsystem for a given interparticle separation. In fact, such pair potential was experimentally measured[22] using optical tweezers, and the results were in agreement with a simple multichain binding model. Later, a conceptually similar model was used to successfully describe experimental data on reversible aggregation and melting in DNA-colloidal systems[24,25] (see **Figure 3**d–e). Multiple refinements of this theory have been proposed over the years.[16,19,22–27] The essential physics of most can be captured with a very basic expression for the two-particle binding free energy:

$$\epsilon = -k_B T N \ln\left(1 + \xi^3 C_0 e^{-\frac{\Delta G}{RT}}\right), \quad (1)$$

where N is the number of complementary single-stranded DNA (ssDNA) pairs that can form a double-stranded DNA (dsDNA) duplex, ΔG is the corresponding hybridization free energy, ξ is a characteristic length scale that is of the order of the thickness of the DNA shell, C_0 is a reference concentration of 1M, k_B is the Boltzmann constant, T is temperature, and R is the ideal gas constant. In this formula, $\xi^3 C_0 e^{-\Delta G/RT}$ represents the hybridization probability. Interestingly, strong binding between two particles is possible even in the regime where this probability is small, given the large number, N, of sticky ssDNA per contact. In fact, this is a typical regime for colloids. Also, the shape of the EP is nearly irrelevant for colloids, since its range is much shorter than the particle size, and they can be viewed as sticky spheres with type-dependent mutual affinity.

In the case of NPs, however, the core size is comparable or even smaller than the size of a DNA shell. Therefore, the applicability of EP is not guaranteed. Nevertheless, this class of models has been shown to have reasonable predictive power. The best known example is the complementary contact model (CCM).[28] It takes into account two key properties of the NP–DNA system: effective size of the particle (represented by the hydrodynamic radius) and DNA coverage. The model postulates that the self-assembled morphology maximizes the relative fraction of hybridized DNA linkers. This simple criterion adequately predicts a number of features of the observed phase diagram. In its core, CCM is closely related to the EP models and similarly favors structures that maximize contact between mutually attractive particles. A number of more recent studies propose a route toward building a full-scale theory further helped by generic algorithms.[29,30]

An alternative to the EP is to describe the DNA with a coarse-grain polymer model.[31–33] Because of the computational complexity, detailed modeling of DNA hybridization is typically not practical, and should be represented either by sticky monomers or other toy models. Even upon this simplification, the simulation of multiple DNA-functionalized particles remains a formidable task. Use of graphics processing unit (GPU)-based computing for molecular dynamics simulations of such NP–DNA systems

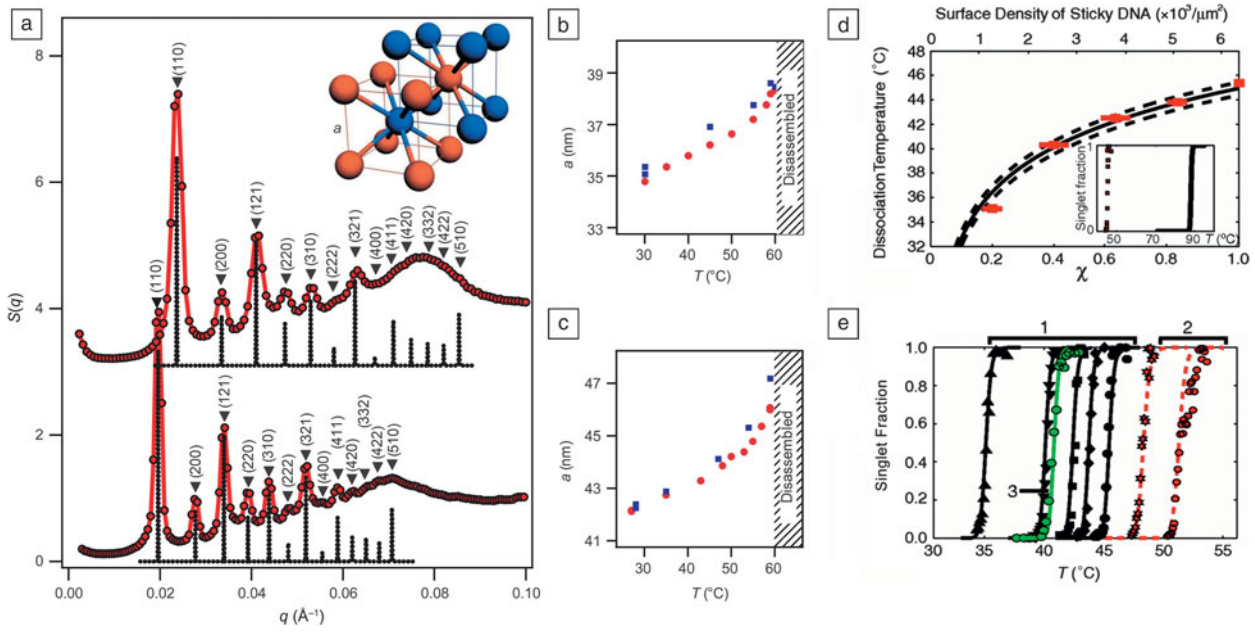


Figure 3. Structural study of assembly and temperature behavior of nanoparticle (NP)–DNA lattices. (a) Small-angle x-ray scattering obtained structure factors for assembled DNA-coated 10-nm gold NP with different DNA shells[13] (a) reveals the body-centered-cubic ordering, as shown in the inset, with (b–c) temperature-dependent lattice constant (*a*). (b–c) Correspond to the systems shown (d); red circles and blue squares are obtained for heating and cooling cycles, respectively. (d–e) Reversible aggregation of DNA-coated colloids for variable composition of DNA shells.[24] Experimental and theoretical dissociation temperature as a function of χ, the fraction of sticky DNA. The red error bars on χ reflect the estimated 10% uncertainty in the coverage. The solid line is the predicted dissociation temperature. Inset: experimental (squares) and theoretical dissociation curves (solid line) before the entropy correction. (e) Melting curves are well described by a simple model, Equation 1; groups 1–3 represent different designs of the DNA linkers. Note: *S*, structure factor; *q*, wave vector transfer; *T*, temperature.

https://doi.org/10.1557/mrs.2016.92 Published online by Cambridge University Press

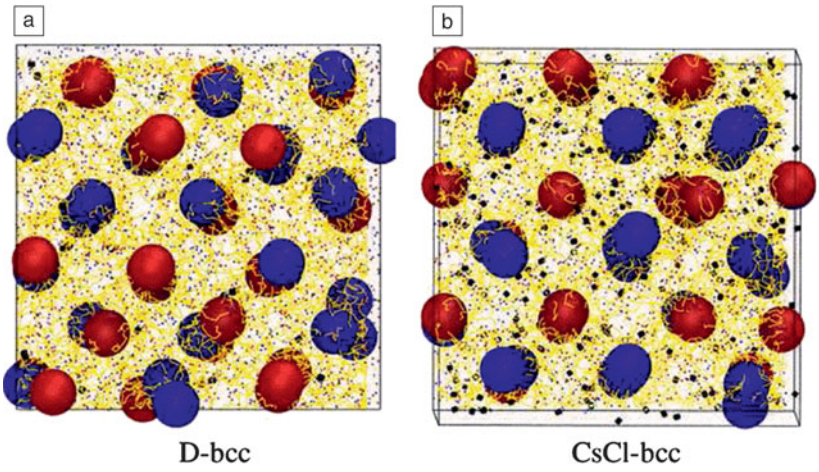


Figure 4. Superlattice self-assembly modeled via graphics processing unit (GPU)-based molecular dynamics simulations. Equilibrated snapshots of (a) "disordered"(body-centered-cubic)-bcc (D-bcc) and (b) CsCl-bcc, with blue and red type nanoparticles and hybridizations (black). Superlattice self-assembly modeled via GPU-based molecular dynamics simulations. Reprinted with permission from Reference 32. © 2011 American Physical Society.

proved to be remarkably efficient. Pioneered by Knorowski et al.[32] (see **Figure 4**a–b for illustration of phase formation), this approach was later used to numerically reproduce experimentally observed superlattices.[33] A promising computational approach is construction of multiscale hybrid models.[34–36] The goal is to construct an analytic multiparticle Hamiltonian through simulation of the DNA-subsystem. Not only does this method produce well-justified pair potentials, it also allows one to take into account the multibody correction to the effective interparticle interactions,[36] essential for NP–DNA systems.

Multicomponent lattices based on spherical particles

One of the most practical ways to achieve greater morphological diversity is to vary the size ratio of the constituent particles.[37,38] This led to the assembly of several types of NP–DNA superlattices. The observed phase behavior has been partially explained by the CCM approach,[39] and it has been further explored in recent studies.[29,30] Pine et al.[5] recently conducted similar studies for micrometer-scale colloids by revealing similarity with NP systems (shown in **Figure 5**a–d) and providing details of phase development.

Successful formation of lattices typically results in a polycrystalline material. Well-defined microcrystals[40] shaped as Wulff polyhedra were successfully generated from DNA-functionalized NPs (Figure 5e–i) grown by a slow-cooling process. This thermodynamically favorable crystal shape is consistent with the crystal structure predicted from theoretical considerations. Due to the presence of the DNA shell, NPs often occupy only <10% by volume of the superlattice. Thus, it is possible to incorporate other components for generating more

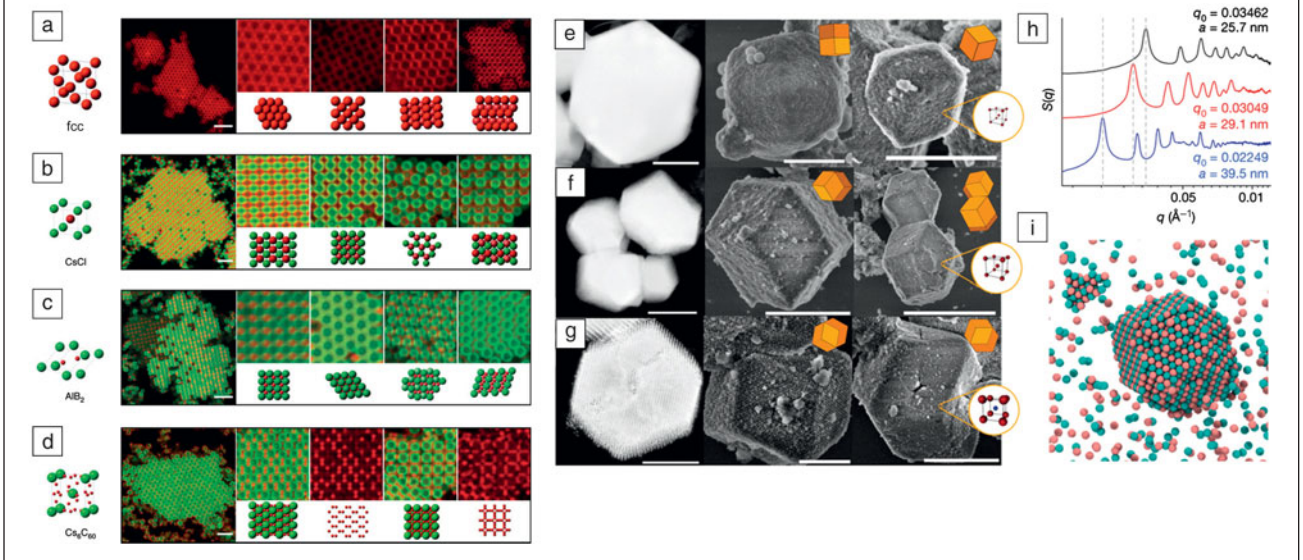


Figure 5. Confocal fluorescent images (scale bar 5 μm) and corresponding drawings of various DNA-coated colloidal crystals: (a) face-centered-cubic (fcc); (b) body-centered-cubic (bcc) (isostructural to CsCl); (c) an AB_2 crystal (isostructural to AlB_2); and (d) an AB_6 crystal lattice (isostructural to Cs_6C_{60}). Reprinted with permission from Reference 5. © 2015 Nature. (e–i) Rhombic dodecahedron microcrystals from gold nanoparticles, (e–g) (left) transmission electron microscope and (middle and right) scanning electron microscope images, (h) small-angle x-ray scattering (SAXS) data, and (i) results of molecular dynamics simulations. Small x-ray scattering provides identification of assembled lattices, while the simulations reveal the assembly mechanism. Note: scale bars, left to right, are (e) 1 μm, 1 μm, and 2 μm; (f) 1 μm, 2 μm, and 4 μm; and (g) 0.5 μm, 1 μm, and 2 μm. Note: *S*, structure factor; *q*, wave vector transfer; q_0, wave vector transfer for the first SAXS peak; *a*, lattice parameter. Reprinted with permission from Reference 40. © 2014 Nature.

https://doi.org/10.1557/mrs.2016.92 Published online by Cambridge University Press

complex three-dimensional (3D) structures, for example, with optical functionalities.[41] Using a basic lattice of DNA-functionalized NPs as a "scaffold," more complex assemblies were achieved by positioning molecular or nanoscale objects in the defined locations, as determined by the DNA encoding.[41,42] In contrast to this incorporation method, a "deletion" of NP inorganic cores has been also demonstrated.[43]

Although gold NPs are often used in the studies, it is clear that the DNA-based platform can facilitate programmable assemblies of different types of particles, so long as they can be coated with DNA. Several approaches were recently demonstrated for generating binary mixtures of NPs with different inorganic cores. For example, bcc superlattices were assembled from an amino-DNA functionalized quantum dot and thiolated-DNA capped gold NP,[44] in which the gold NPs were positioned in a simple cubic manner. Generally applicable carboxylic-based conjugation[44,45] and click-chemistry[46–49] approaches to functionalize NPs with DNA have been developed.

Using these methods, a broad range of functional NPs, including plasmonic, magnetic (iron oxide), catalytic (palladium), and luminescent (cadmium selenite, cadmium telluride) NPs were assembled into heterogeneous superlattices. It was found that the particle shape difference could suppress structural ordering, but the effect is minimized for larger ssDNA shells.[45] Interestingly, the multicomponent lattices can exhibit compositional disorder for soft DNA shells; a progressive decrease of structural order and transition to clustering was also observed for small grafting numbers.[45] Novel optical and field-responsive properties of the DNA-assembled multicomponent materials were demonstrated as well.

Assembly of anisotropic particles

Particle shapes have profound effects on the type of formed structures, even for solid objects.[50] Assembly of DNA-functionalized NPs of different shapes, including rods, triangular prisms, octahedra, and rhombic dodecahedra, can result in the formation of dense phases in which particles maximize interactions of complementary rigid chains.[51] For example, prisms form linear arrays, while rods form hexagonally packed membranes. Such organizations resemble the phases observed for solid objects. However, the polymeric nature of DNA chains can also induce unexpected assembly pathways. For example, it was observed that one-dimensional ladder-like ribbon structures emerge due to the spontaneous symmetry breaking of interparticle interactions during assembly of radially isotropic DNA-decorated nanoscale rods.[7] Similar linear structures of alternating rods and spheres were also observed, indicating that collective effects of flexible linkers might promote new structural organizations.

Recent studies also demonstrated that both shape complementary and noncomplementary scenarios can be realized for assembly of dissimilar shapes into unified lattices with the help of DNA in binary mixtures (**Figure 6**a–c).[6,52] Although traditionally the shape difference would be expected to lead to phase separation, the complementarity between DNA on particles of different shapes allows for co-assembly. If the shapes have overall similar symmetry, the original phase is preserved even if the shapes are somewhat modulated, as was shown for nanocubes.[52] However, for mixtures of anisotropic (nanocubes, octahedra) and spherical NPs, the anisotropic particle dictates the phase behavior,[6] while a certain softness of shells is required to accommodate the shape disparity. Such an approach permits designing lattice formation by the introduction of well-defined geometrical elements that impose specific binding coordination between particles, and where local symmetry correlates with the resulting self-assembled lattice. This idea was further demonstrated for the creation of designed low-dimensional lattices using DNA origami octahedra, 3D frame made out of folded DNA, as shaped interparticle linkers.[53]

Recently, a new lattice assembly strategy was introduced[54,55] based on the use of DNA frames, which are complex 3D DNA constructs[56] that can prescribe the topology of interparticle connections.[53] These nontrivial building blocks, specifically designed DNA frames of different shapes, can be used as multiparticle connectors and as particle cages;[57,58] thus, they can dictate the desired anisotropic interactions without the complexity of particle design and without the necessity of changing particles for obtaining the targeted lattices. The diverse range of structures assembled using this strategy includes the diamond family of superlattices[54] (**Figure 7**a–c), traditionally considered an iconic challenge in colloidal self-assembly, as well as other rationally assembled lattices based on the polyhedral frames.[55] Such an approach opens a new frontier in the creation of designed NP lattices with DNA.

Stimuli responsive superlattices

Dynamically reconfigurable superlattices can be implemented by using flexible ssDNA as a linker. In one study, osmotic pressure was shown to compress the NP–DNA lattice by as much

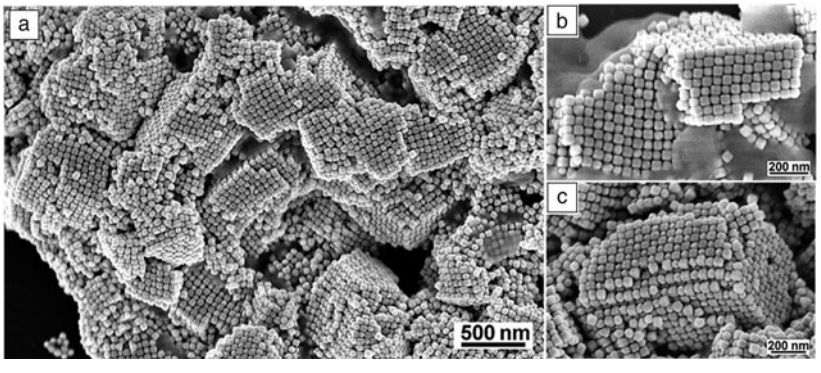


Figure 6. (a–c) Self-assembly of cubic lattice isostructural to NaCl for DNA-functionalized nanocubes and nanospheres.[6]

https://doi.org/10.1557/mrs.2016.92 Published online by Cambridge University Press

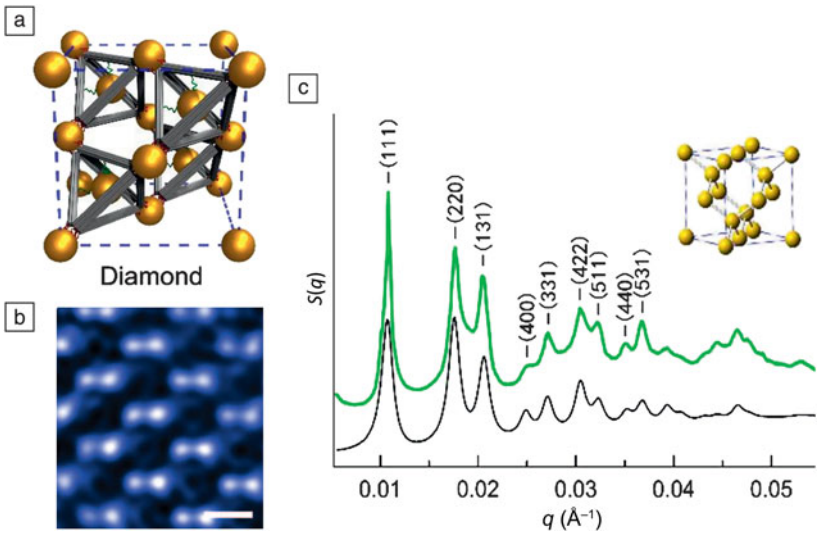


Figure 7. Assembly of a diamond lattice from DNA-coated gold nanoparticles and tetrahedral DNA origami frames. (a) Schematic of the structure; (b) scanning transmission electron microscope image, scale bar is 50 nm; and (c) small-angle x-ray scattering (SAXS) obtained structure factor $S(q)$ and (inset) a model of diamond lattice are shown.[54] Green and black curves correspond to experimental and modeled structure factors, respectively. Excellent agreement between them confirm the assembly of the diamond structure. Note: A and B, particles coated with respectively complementary DNA; S, structure factor; q, wave vector transfer; q_0, wave vector transfer for the first SAXS peak.

as six times in volume, without destroying its order.[59] Salt concentration[41,60,61] and hydration[62] are environmental parameters for controlling the crystallization and lattice constants of superlattices. Moreover, triggering a transformation of the two-dimensional NP system from a hexagonal lattice to string-like clusters and to a weakly ordered network has been observed and correlated with changed rheological properties of the monolayer.[63]

Highly specific responses to external stimuli have been explored in the case where NPs in a lattice were linked with a switchable DNA "device."[64] The lattice constant of a bcc crystal was modulated by about 25% by adding specific DNA strands that alter the device state between two crystalline configurations.[64,65] In a recent study, a molecular intercalation-based strategy was demonstrated for the reversible extension of dsDNA-linked NP lattices by ~30%, using ethedium bromide as the intercalator molecule.[66] Such regulation of interparticle distances can be used to modulate coupling between NPs for applications in plasmonic, light-emitting, and magnetic materials.

There is significant interest in creating dynamic lattices that can change their global organizational properties, such as for creating materials with switchable functions. Colloidal particles interacting through DNA linkers can be designed to form solids that melt when either heated or cooled;[67] also, reentrant melting and arbitrarily wide gas–solid transition were demonstrated experimentally.[68] These advances will permit, for example, creating materials with unique mechanical responses to temperature.

Recently, an intriguing concept of programmable switching of the crystallographic symmetry of an entire NP lattice into different phases by tailoring *in situ* interparticle interactions was proposed and implemented.[69] Reversible transformations can also be achieved by designing DNA shell modifications.[70] These studies demonstrate that targeted modification of NP shells allows for reprogramming of interactions in a dynamical manner, resulting in a series of phase transitions. This result opens up opportunities for creating systems whose structures and functions can be changed on demand. A combined diversity of particle types can be integrated using DNA methods, [7,45,46,51] advances in DNA functionalization of particles,[45–48,71] and to potentially generate novel strategies for the lattice design[5,6,28,30,54,55] a broad range of materials with desired performances.

Conclusions

In recent years, a new powerful approach based on DNA-driven particle interactions was demonstrated for and applied to the creation of ordered particle arrays. Programmable interactions provided by complementary DNA strands offer incorporation of multiple particle types, tunability of binding characteristics through the tailored design of DNA shells, and ample capabilities for structure reconfigurations. Significant progress was achieved in DNA-guided assembly of superlattices built from micrometer and nanoscale particles of different sizes, shapes, and chemical compositions. Moreover, by modulating the structure of DNA shells, nanoparticle shapes, and the topology of linking constructs, diverse lattice types were observed. While we are far from completely understanding these systems and predicting their phases, both experimental and theoretical efforts demonstrate enormous progress in revealing the leading parameters determining structure formation in these systems. Recent success in coupling complex DNA constructs and DNA-coated NPs into integral architectures reassures that in the near future, self-assembly for NP–DNA lattices might reach a new level of control. DNA-based strategies will allow for the assembly of desired targeted architectures. These advances in assembly of 3D particle arrays can be directly applied to fabrication of new types of materials from functional particles, thus enabling the full-scale engineering of desired optical, magnetic, and bio-related functions.

Acknowledgment

Research was carried out at the Center for Functional Nanomaterials, Brookhaven National Laboratory, and is supported by the US Department of Energy, Office of Basic Energy Sciences, under Contract No. DE-SC0012704.

https://doi.org/10.1557/mrs.2016.92 Published online by Cambridge University Press

References

1. A. Klinkova, R.M. Choueiri, E. Kumacheva, *Chem. Soc. Rev.* **43**, 3976, doi:10.1039/c3cs60341e (2014).
2. J.Y. Wang, C. Song, J.K. Xu, B.Q. Ding, *Prog. Chem.* **24**, 1936 (2012).
3. W.B. Rogers, W.M. Shih, V.N. Manoharan, *Nat. Rev. Mater.* **1**, 16008 (2016), doi:10.1038/natrevmats.2016.8.
4. M.T. Casey, R.T. Scarlett, W.B. Rogers, I. Jenkins, T. Sinno, J.C. Crocker, *Nat. Commun.* **3**, 1209 (2012), doi:10.1038/ncomms2206.
5. Y. Wang, Y. Wang, X. Zheng, E. Ducrot, J.S. Yodh, M. Weck, D.J. Pine, *Nat. Commun.* **6**, 7253 (2015).
6. F. Lu, K.G. Yager, Y.G. Zhang, H.L. Xin, O. Gang, *Nat. Commun.* **6**, 6912 (2015), doi:10.1038/ncomms7912.
7. S. Vial, D. Nykypanchuk, K.G. Yager, A.V. Tkachenko, O. Gang, *ACS Nano* **7**, 5437 (2013), doi:10.1021/nn401413b.
8. A.P. Alivisatos, K.P. Johnsson, X.G. Peng, T.E. Wilson, C.J. Loweth, M.P. Bruchez, P.G. Schultz, *Nature* **382**, 609 (1996).
9. C.A. Mirkin, R.L. Letsinger, R.C. Mucic, J.J. Storhoff, *Nature* **382**, 607 (1996).
10. M.P. Valignat, O. Theodoly, J.C. Crocker, W.B. Russel, P.M. Chaikin, *Proc. Natl. Acad. Sci. U.S.A.* **102**, 4225 (2005).
11. M.M. Maye, D. Nykypanchuk, D. van der Lelie, O. Gang, *Small* **3**, 1678 (2007).
12. A.J. Kim, P.L. Biancaniello, J.C. Crocker, *Langmuir* **22**, 1991 (2006).
13. D. Nykypanchuk, M.M. Maye, D. van der Lelie, O. Gang, *Nature* **451**, 549 (2008).
14. H.M. Xiong, D. van der Lelie, O. Gang, *J. Am. Chem. Soc.* **130**, 2442 (2008).
15. S.Y. Park, A.K.R. Lytton-Jean, B. Lee, S. Weigand, G.C. Schatz, C.A. Mirkin, *Nature* **451**, 553 (2008).
16. A.V. Tkachenko, *Phys. Rev. Lett.* **89**, 148303 (2002).
17. K.T. Wu, L. Feng, R.J. Sha, R. Dreyfus, A.Y. Grosberg, N.C. Seeman, P.M. Chaikin, *Proc. Natl. Acad. Sci. U.S.A.* **109**, 18731 (2012).
18. H.M. Xiong, D. van der Lelie, O. Gang, *Phys. Rev. Lett.* **102**, 015504 (2009).
19. S. Angioletti-Uberti, P. Varilly, B.M. Mognetti, A.V. Tkachenko, D. Frenkel, *J. Chem. Phys.* **138**, 021102 (2013).
20. L. Di Michele, F. Varrato, J. Kotar, S.H. Nathan, G. Foffi, E. Eiser, *Nat. Commun.* **4**, 2007 (2013).
21. F. Varrato, L. Di Michele, M. Belushkin, N. Dorsaz, S.H. Nathan, E. Eiser, G. Foffi, *Proc. Natl. Acad. Sci. U.S.A.* **109**, 19155 (2012).
22. P. Biancaniello, A. Kim, J. Crocker, *Phys. Rev. Lett.* **94**, 94 (2005).
23. N.A. Licata, A.V. Tkachenko, *Phys. Rev. E* **74**, 041408 (2006).
24. R. Dreyfus, M.E. Leunissen, R.J. Sha, A.V. Tkachenko, N.C. Seeman, D.J. Pine, P.M. Chaikin, *Phys. Rev. Lett.* **102**, 048301 (2009).
25. R. Dreyfus, M.E. Leunissen, R. Sha, A. Tkachenko, N.C. Seeman, D.J. Pine, P.M. Chaikin, *Phys. Rev. E* **81**, 041404 (2010).
26. P. Varilly, S. Angioletti-Uberti, B.M. Mognetti, D. Frenkel, *J. Chem. Phys.* **137**, 094108 (2012).
27. W.B. Rogers, J.C. Crocker, *Proc. Natl. Acad. Sci. U.S.A.* **108**, 15687 (2011).
28. R.J. Macfarlane, B. Lee, M.R. Jones, N. Harris, G.C. Schatz, C.A. Mirkin, *Science* **334**, 204 (2011).
29. B. Srinivasan, T. Vo, Y.G. Zhang, O. Gang, S. Kumar, V. Venkatasubramanian, *Proc. Natl. Acad. Sci. U.S.A.* **110**, 18431 (2013).
30. T. Vo, V. Venkatasubramanian, S. Kumar, B. Srinivasan, S. Pal, Y.G. Zhang, O. Gang, *Proc. Natl. Acad. Sci. U.S.A.* **112**, 4982 (2015).
31. B.M. Mladek, J. Fornleitner, F.J. Martinez-Veracoechea, A. Dawid, D. Frenkel, *Phys. Rev. Lett.* **108**, 268301 (2012).
32. C. Knorowski, S. Burleigh, A. Travesset, *Phys. Rev. Lett.* **106**, 215501 (2011).
33. T.I.N.G. Li, R. Sknepnek, R.J. Macfarlane, C.A. Mirkin, M.O. de la Cruz, *Nano Lett.* **12**, 2509 (2012).
34. M.E. Leunissen, D. Frenkel, *J. Chem. Phys.* **134**, 084702 (2011).
35. F.J. Martinez-Veracoechea, B.M. Mladek, A.V. Tkachenko, D. Frenkel, *Phys. Rev. Lett.* **107**, 045902 (2011).
36. B.M. Mladek, J. Fornleitner, F.J. Martinez-Veracoechea, A. Dawid, D. Frenkel, *Soft Matter* **9**, 7342 (2013).
37. M.E. Leunissen, C.G. Christova, A.P. Hynninen, C.P. Royall, A.I. Campbell, A. Imhof, M. Dijkstra, R. van Roij, A. van Blaaderen, *Nature* **437**, 235 (2005).
38. E.V. Shevchenko, D.V. Talapin, N.A. Kotov, S. O'Brien, C.B. Murray, *Nature* **439**, 55 (2006).
39. R.J. Macfarlane, M.R. Jones, A.J. Senesi, K.L. Young, B. Lee, J.S. Wu, C.A. Mirkin, *Angew. Chem. Int. Ed.* **49**, 4589 (2010).
40. E. Auyeung, T.I.N.G. Li, A.J. Senesi, A.L. Schmucker, B.C. Pals, M.O. de la Cruz, C.A. Mirkin, *Nature* **505**, 73 (2014).
41. H.M. Xiong, M.Y. Sfeir, O. Gang, *Nano Lett.* **10**, 4456 (2010).
42. R.J. Macfarlane, M.R. Jones, B. Lee, E. Auyeung, C.A. Mirkin, *Science* **341**, 1222 (2013).
43. E. Auyeung, J.I. Cutler, R.J. Macfarlane, M.R. Jones, J.S. Wu, G. Liu, K. Zhang, K.D. Osberg, C.A. Mirkin, *Nat. Nanotechnol.* **7**, 24 (2012).
44. D.Z. Sun, O. Gang, *J. Am. Chem. Soc.* **133**, 5252 (2011).
45. Y.G. Zhang, F. Lu, K.G. Yager, D. van der Lelie, O. Gang, *Nat. Nanotechnol.* **8**, 865 (2013).
46. C. Zhang, R.J. Macfarlane, K.L. Young, C.H.J. Choi, L.L. Hao, E. Auyeung, G.L. Liu, X.Z. Zhou, C.A. Mirkin, *Nat. Mater.* **12**, 741 (2013).
47. Y.F. Wang, Y. Wang, X.L. Zheng, E. Ducrot, M.G. Lee, G.R. Yi, M. Weck, D.J. Pine, *J. Am. Chem. Soc.* **137**, 10760 (2015).
48. A. Heuer-Jungemann, R. Kirkwood, A.H. El-Sagheer, T. Brown, A.G. Kanaras, *Nanoscale* **5**, 7209 (2013).
49. https://en.wikipedia.org/wiki/click_chemistry.
50. P.F. Damasceno, M. Engel, S.C. Glotzer, *Science* **337**, 453 (2012).
51. M.R. Jones, R.J. Macfarlane, B. Lee, J. Zhang, K.L. Young, A.J. Senesi, C.A. Mirkin, *Nat. Mater.* **9**, 913 (2010).
52. M.N. O'Brien, M.R. Jones, B. Lee, C.A. Mirkin, *Nat. Mater.* **14**, 833 (2015).
53. Y. Tian, T. Wang, W.Y. Liu, H.L. Xin, H.L. Li, Y.G. Ke, W.M. Shih, O. Gang, *Nat. Nanotechnol.* **10**, 637 (2015).
54. W. Liu, M. Tagawa, H.L. Xin, T. Wang, H. Emamy, H. Li, K.G. Yager, F.W. Starr, A.V. Tkachenko, O. Gang, *Science* **351**, 582 (2016).
55. Y. Tian, Y. Zhang, T. Wang, H.L. Xin, H. Li, O. Gang, *Nat. Mater.*, published online February 22, 2016, http://dx.doi.org/10.1038/nmat4571.
56. S.M. Douglas, H. Dietz, T. Liedl, B. Hogberg, F. Graf, W.M. Shih, *Nature* **459**, 414 (2009).
57. N.A. Licata, A.V. Tkachenko, *Phys. Rev. E* **79**, 011404 (2009).
58. Y.L. Li, Z.Y. Liu, G.M. Yu, W. Jiang, C.D. Mao, *J. Am. Chem. Soc.* **137**, 4320 (2015).
59. S. Srivastava, D. Nykypanchuk, M.M. Maye, A.V. Tkachenko, O. Gang, *Soft Matter* **9**, 10452 (2013).
60. S.J. Tan, J.S. Kahn, T.L. Derrien, M.J. Campolongo, M. Zhao, D.-M. Smilgies, D. Luo, *Angew. Chem. Int. Ed.* **53**, 1316 (2014).
61. S. Srivastava, D. Nykypanchuk, M. Fukuto, O. Gang, *ACS Nano* **8**, 9857 (2014).
62. B. Radha, A.J. Senesi, M.N. O'Brien, M.X. Wang, E. Auyeung, B. Lee, C.A. Mirkin, *Nano Lett.* **14**, 2162 (2014).
63. S. Srivastava, D. Nykypanchuk, M. Fukuto, J.D. Halverson, A.V. Tkachenko, K.G. Yager, O. Gang, *J. Am. Chem. Soc.* **136**, 8323 (2014).
64. M.M. Maye, M.T. Kumara, D. Nykypanchuk, W.B. Sherman, O. Gang, *Nat. Nanotechnol.* **5**, 116 (2010).
65. Y. Kim, R.J. Macfarlane, C.A. Mirkin, *J. Am. Chem. Soc.* **135**, 10342 (2013).
66. S. Pal, Y. Zhang, S.K. Kumar, O. Gang, *J. Am. Chem. Soc.* **137**, 4030 (2015).
67. S. Angioletti-Uberti, B.M. Mognetti, D. Frenkel, *Nat. Mater.* **11**, 518 (2012).
68. W.B. Rogers, V.N. Manoharan, *Science* **347**, 639 (2015).
69. Y. Zhang, B. Srinivasan, T. Vo, S. Pal, S. Kumar, O. Gang, *Nat. Mater.* **14**, 840 (2015).
70. Y. Kim, R.J. Macfarlane, M.R. Jones, C.A. Mirkin, *Science* **351**, 579 (2016).
71. D.Z. Sun, O. Gang, *Langmuir* **29**, 7038 (2013). □



https://doi.org/10.1557/mrs.2016.92 Published online by Cambridge University Press